RARE METALS
Vol. 28, No. 5, Oct 2009, p. 511
DOI: 10.1007/s12598-009-0099-y

Effects of trace Zr on the microstructure and properties of 2E12 alloy

WANG Jianzhao[a], FANG Canfeng[a], HAO Hai[a], WANG Shaohua[a], YANG Shoujie[b], DAI Shenglong[b], and ZHANG Xingguo[a]

[a] *School of Materials Science and Engineering, Dalian University of Technology, Dalian 116024, China*
[b] *Beijing Institute of Aeronautical Materials, Beijing 100095, China*

Received 14 September 2008; received in revised form 18 November 2008; accepted 21 November 2008

Abstract

Al-4.0Cu-1.4Mg-0.6Mn (2E12) and Al-4.0Cu-1.4Mg-0.6Mn-0.3Zr aluminum billets were manufactured by soft-contact electromagnetic continuous casting (EMC). Subsequent forging and heat treatment were conducted and the effects of Zr on the microstructure and properties of the Al-4.0Cu-1.4Mg-0.6Mn alloy were studied. The results show that the addition of 0.3% Zr can reduce the dendrite and refine grains. During forging and solution treatment, fine and dispersive Al_3Zr particles precipitated from the supersaturated α (Al) solid solution in the heating process of the billet can effectively pin dislocations and subgrain boundaries. Because of the addition of Zr, the mechanical properties are improved with the tensile strength, yield strength, elongation, and contraction of the area increasing by 5.4%, 11.3%, 9.7%, and 12.6%, respectively. Moreover, under the condition of R = 0.1, the fatigue crack growth rate (da/dN) of the Al-4.0Cu-1.4Mg-0.6Mn-0.3Zr alloy is lower than that of the Al-4.0Cu-1.4Mg-0.6Mn alloy.

Keywords: aluminum alloy; heat treatment; microstructure; mechanical properties; fatigue crack growth rate

1. Introduction

Aluminum alloys have widespread application and an irreplaceable position in the areas of aerospace and nuclear industries. Therefore, technologies related to aluminum alloys are regarded as the key and supporting technology of national defense [1-2]. 2E12 alloy, which was developed on the basis of 2A12 (2024) alloy by decreasing the contents of Fe and Si, has fine fracture toughness, fatigue and stress corrosion resistance [3-5]. As the best skin material, this alloy was first used in the Boeing 777 aircraft and recently applied in the A380 large passenger plane [6-7]. The leading strengthening phases of this alloy are S (Al_2CuMg) and θ (Al_2Cu). 2E12 alloy is usually used under 100°C; otherwise, its strength reduces obviously because of the coarsening of the strengthening phases [8]. Micro-alloying is the main method to improve the properties of 2E12 alloy besides heat treatment. Frindlyander, a scholar from the former Soviet Union, first added Zr into aluminum alloys in 1956 [9]. Further, the effects of Zr on the microstructure and properties of Al-Zn-Mg-Cu alloys were widely studied. The studies indicated that trace Zr could refine the microstructure and increase strength and temperature of recrystallization.

The effects of Zr on 2E12 alloy prepared by soft-contact electromagnetic continuous casting have been studied, but the study on forging of 2E12 alloy under T4 treatment is unreported up to now. In this paper, the effects of Zr on the fatigue crack growth rate, mechanical properties, and microstructure of 2E12 alloy forgings under T4 treatment are studied. Moreover, the effects of Zr on the natural and artificial age-hardenings of 2E12 alloy are investigated.

2. Experimental

Al-4Cu-1.4Mg-0.6Mn (2E12) and Al-4Cu-1.4Mg-0.6Mn-0.3Zr were manufactured by soft-contact electromagnetic continuous casting (EMC), and their compositions are shown in Table 1. The parameters of EMC were as fol-

Table 1. Chemical composition of the alloys wt.%

Alloy	Cu	Mg	Mn	Zr	Fe	Si	Al
Alloy 1 (Al-4Cu-1.4Mg-0.6Mn)	4.10	1.45	0.55	—	<0.06	<0.06	Bal.
Alloy 2 (Al-4Cu-1.4Mg-0.6Mn-0.3Zr)	4.08	1.47	0.54	0.30	<0.06	<0.06	Bal.

Corresponding author: ZHANG Xingguo **E-mail:** zxgwj@dlut.edu.cn

lows: the frequency of electromagnetic field, the pouring temperature, the flow rate of cooling-water, and the casting speed were 2500 Hz, 710-730°C, 1.8 m^3/h, and 3×10^{-3} m/s, respectively.

The samples with a size of ϕ110 mm × 150 mm were taken from the same position of the billets. The alloy under T4 heat treatment was finally obtained by uniform heat treatment (490°C, 10 h), free forging, solution treatment (495°C, 1 h), water quenching (transfer time less than 15 s), and natural aging (96 h). The flow chart of free forging is shown in Fig. 1. Besides, the temperature of artificial age-hardening was 190°C.

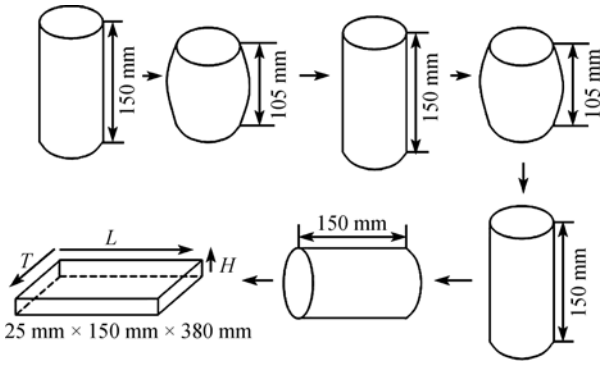

Fig. 1. Flow chart of free forging.

Metallographic specimens were prepared by the standard procedure and etched in a solution of 2 mL HF + 3 mL HCl + 5 mL HNO_3 + 200 mL H_2O. The microstructure was observed by multifunction optical microscopy. The hardness values at different times of natural and artificial aging processes were measured with a light loaded durometer, and the magnitude of the load was 1000 kN with 30 s loading time. The tensile properties in the *L* direction of the alloys under T4 condition were measured with an electro universal test machine. The fatigue crack growth rate of the alloys were examined from GB/T 6398—2000 under the condition of $R = 0.1$ (R is the ratio of the minimum to maximum stresses under cyclic loading) and $f = 10$ Hz, and da/dN was the quantity of fatigue crack growth in one cycle of load. The fractures were observed by scanning electron microscopy.

3. Results and discussion

3.1. Microstructure of the alloys

The microstructure of alloys 1 and 2 is shown in Fig. 2. The as-cast microstructure of alloy 1 is dominated by uniform grains, whose mean size is about 40 μm as shown in Fig. 2(a), because of electromagnetic stirring, but dendritic structures are clearly observed. According to the energy spectrum analysis of SEM, the leading strengthening phases, S (Al_2CuMg) and θ (Al_2Cu), mainly distribute in the grain boundaries. As shown in Fig. 2(c), the microstructure is characterized by refined equiaxed grains with a size of 30 μm with the addition of 0.3% Zr. The results show that a micro addition of Zr can reduce the dendritic structures and refine the as-cast microstructure obviously.

Fig. 2(b) and Fig. 2(d) show the forging microstructure of alloys 1 and 2 under T4 treatment. The grains of alloy 1 grow coarsely as a result of recrystallization, whereas the grains of alloy 2 are slender and uniform because of Al_3Zr, generated by Zr and Al, which could inhibit recrystallization and keep the stabilization of alloys under high temperature.

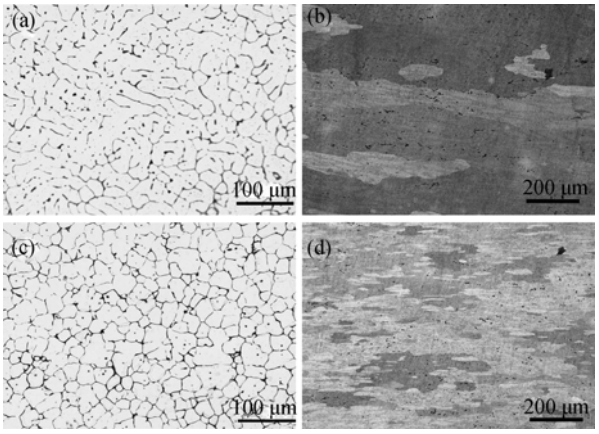

Fig. 2. Optical micrographs of the alloys: (a) as-cast microstructure of alloy 1; (b) microstructure of alloy 1 under T4 condition; (c) as-cast microstructure of alloy 2; (d) microstructure of alloy 2 under T4 condition.

3.2. Age-hardening curves of the alloys

The natural and artificial age-hardening curves of alloy 1 and alloy 2 are shown in Fig. 3. The natural age-hardening curves of the two alloys stay consistent approximately, so it is obvious that the addition of 0.3% Zr has little effect on the process of natural age-hardening of 2E12 alloy. In the process of artificial age-hardening, the peak-aging of alloy 1 locates at 6-14 h while that of alloy 2 appears after 10 h and lasts up to 24 h. The results show that the addition of Zr extends the peak-aging time of artificial age-hardening at 190°C. The main reason is that the Al_3Zr dispersoids which separate out in the grain boundary can retard the movement of dislocations.

3.3. Tensile properties of the alloys under T4 treatment

The tensile properties of the alloys under T4 treatment are shown in Table 2. With the micro addition of Zr, the tensile properties of alloy 2 are improved with tensile strength, yield strength, elongation, and reduction of area increasing by 5.4%, 11.3%, 9.7%, and 12.6%, respectively. The strengthening mechanisms of the alloy are mainly

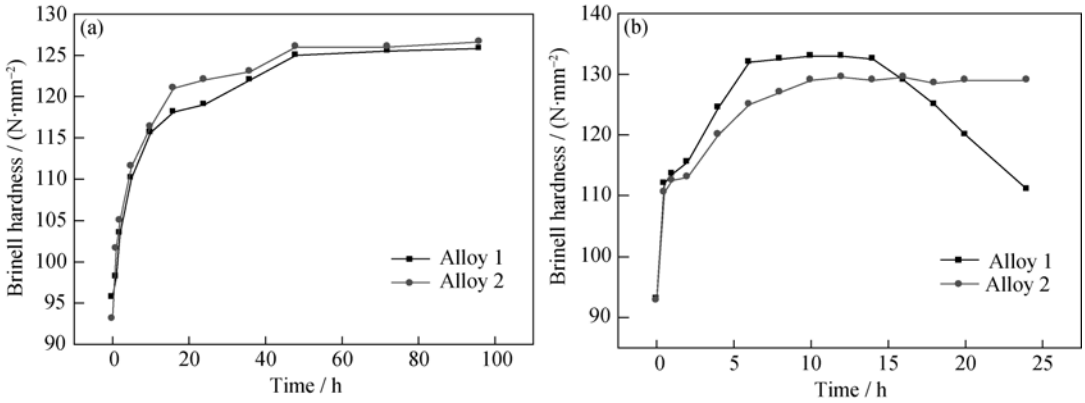

Fig. 3. Age-hardening curves of the alloys: (a) natural aging; (b) artificial aging.

Table 2. Effects of Zr on the tensile properties of the alloys

Alloy	σ_b / MPa	$\sigma_{p0.2}$ / MPa	δ / %	ψ / %
Alloy 1	445	282	20.6	27.7
Alloy 2	469	314	22.6	31.2

fine-grained strengthening, solution strengthening, and mechanical hardening. Two grain refinements are present: refinement of the grains of the billet during casting; refinement of recrystal grains or subgrains by the localization effect of Al_3Zr after forging.

The fine-grained strengthening includes two parts.

According to the Hall-Petch formula:

$$\sigma = \sigma_0 + K \cdot d^{-1/2} \quad (1)$$

where σ is the yield strength of the alloy, MPa; σ_0 is the yield strength of a single crystal, MPa; d is the average diameter of multiple crystals, mm; and K is a constant attributed the influence level of grain boundary to strength. According to Eq. (1), the yield strength increases with a decrease in grain size.

Al_3Zr particles whose microhardnesses are greater than 5000 MPa separate out during the uniform heat treatment and hot-working treatment. Al_3Zr particles produce a dispersion strengthening effect because these particles are hardly dissolved. Moreover, a number of dislocations and fibrous tissues which generate in the deformation process have great deforming strengthening effect.

Fig. 4 shows the tensile fracture appearances. The fracture of alloy 1 with less dimples and breaking particles observed in the dimples platform shows the low gliding fracture characteristic, whereas the fracture of alloy 2 shows the typical ductile fracture characteristic. With the addition of 0.3% Zr, the fracture of alloy 2 shows evenly distributed dimples which are more and smaller than that of alloy 1.

3.4. Fatigue crack growth rate of the alloys under T4 treatment

Fig. 5 shows the fatigue crack growth rate of the alloys. Under the condition of stress ratio $R = 0.1$, the fatigue crack growth rate curves of the two alloys have obvious three-stage characteristic and similar tendency in *T-L* direction. When ΔK is less than 9 MPa·m$^{1/2}$, from 9 to 27 MPa·m$^{1/2}$, and more than 27 MPa·m$^{1/2}$, both alloys are in the microscopic cracking stage, macroscopic cracking

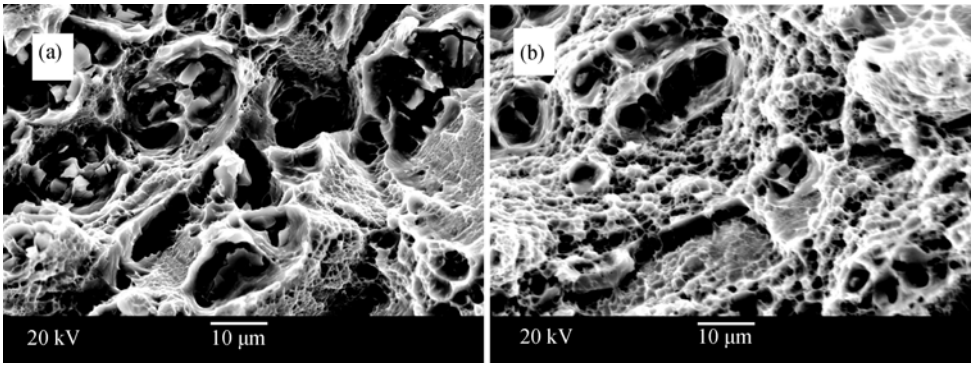

Fig. 4. Fracture appearances of alloy 1 (a) and alloy 2 (b) under T4 condition.

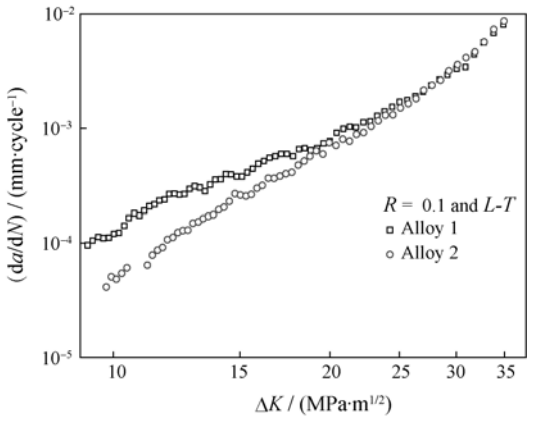

Fig. 5. Fatigue crack growth rate of the alloys.

steady-state expansion stage, and fast fracture stage, respectively. The fatigue crack growth rate of alloy 2 is lower than that of alloy 1. The result shows that the addition of Zr can improve the fatigue durability of 2E12 alloy.

Fig. 6 shows the fracture appearances of fatigue crack growth of the two alloys. Crystallographic expansion of cracks or dissociation facets is observed from the fracture appearances of the first stage as shown in Figs. 6(a) and 6(e). Figs. 6(b) and 6(f) show the fracture appearances of the beginning of the second stage, which have clear fatigue striation characteristic. The space lengths of fatigue striations of alloys 1 and 2 are 2-3 and 1-2 μm, respectively. The fatigue durability of alloy 2 is better than that of alloy 1 because of the thinner fatigue striations. Figs. 6(c) and 6(g) are the fracture appearances of the anaphase of the macroscopic cracking expansion stage. The fatigue crack growth rate of the alloys here has obvious increment compared with the initial stage of fatigue crack growth. Fracture appearances only have a few fatigue striations and static fracture failure modes such as the dissociation and intergranular crack mode. These static fracture modes could greatly increase the sensibility of fatigue crack growth as to the microstructure. The instant fracture stage has gliding fracture characteristic as shown in Figs. 6(d) and 6(h). The fracture appearance of this stage, which has lots of dimples, is similar to the tensile fracture appearance. There are second-phase particles in the dimples and some of these particles are breaking. Compared with 2024 alloy, 2E12 alloy has a better fatigue durability when the strength has little change because the lower contents of Fe and Si decrease the quantities of coarse brittle impurity phases.

4. Conclusions

(1) The as-cast microstructure of 2E12 alloy can be refined with grain sizes decreasing from 42 to 30 μm with the addition of 0.3% Zr and characterized with equiaxed grains. Moreover, recrystallization during the forging process can be inhibited and the microstructure of T4 heat treatment billets has an obvious improvement.

(2) The addition of 0.3% Zr has little effect on the process of natural age-hardening of 2E12 alloy, but it can extend the peak-aging time of artificial age-hardening at 190°C.

(3) With an addition of 0.3% Zr, the mechanical properties of 2E12 alloy are improved with the tensile strength, yield strength, elongation, and reduction of area increasing by 5.4%, 11.3%, 9.7%, and 12.6%, respectively.

(4) Under the condition of R = 0.1, the fatigue crack growth rate (da/dN) of the Al-4.0Cu-1.4Mg-0.6Mn-0.3Zr alloy is lower than that of the Al-4.0Cu-1.4Mg-0.6Mn (2E12) alloy. The addition of 0.3% Zr can improve the fatigue durability of 2E12 alloy.

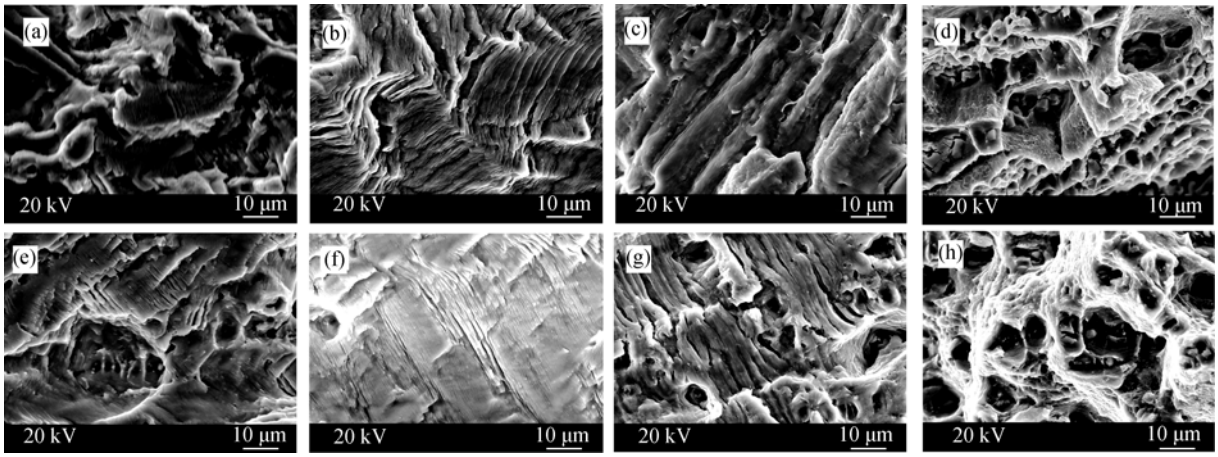

Fig. 6. Fatigue fracture surfaces of the alloys (R = 0.1): (a) ΔK = 9 MPa·m$^{1/2}$ (alloy 1); (b) ΔK = 12 MPa·m$^{1/2}$ (alloy 1); (c) ΔK = 25 MPa·m$^{1/2}$ (alloy 1); (d) ΔK = 30 MPa·m$^{1/2}$ (alloy 1); (e) ΔK = 9 MPa·m$^{1/2}$ (alloy 2); (f) ΔK = 12 MPa·m$^{1/2}$ (alloy 2); (g) ΔK = 25 MPa·m$^{1/2}$ (alloy 2); (h) ΔK = 30 MPa·m$^{1/2}$ (alloy 2).

References

[1] Heinz A., Haszler A., Keidel C., Moldenhauer S., Benedictus R., and Miller W.S., Recent development in aluminum alloys for aerospace application, *Mater. Sci. Eng. A*, 2000, **280** (1): 102.

[2] Staley J.T., Liu J., and Hunt W., Aluminum alloys for aerostructures, *Adv. Mater. Processes*, 1997, **152** (4): 17.

[3] Cassada W., Liu J., and Staley J., Aluminum alloys for aircraft structure, *Adv. Mater. Processes*, 2002, **160** (12): 27.

[4] Iau J. and Kulak M., A new paradigm in the design of aluminum alloys for aerospace applications, *Mater. Sci. Forum*, 2000, **331/337**: 127.

[5] ASTM, Standard test method for exfoliation corrosion susceptibility in 2xxx and 7xxx series aluminum alloys (EXCO test), USA, 1985.

[6] Nakai M. and Eto T., New aspects of development of high strength aluminum alloys for aerospace applications, *Mater. Sci. Eng. A*, 2000, **285** (1): 62.

[7] Starke E.A. Jr and Staleyt J.T., Application of modern aluminum alloys to aircraft, *Prog. Aerospace Sci.*, 1996, **32** (2-3): 131.

[8] Polmear I.J. and Couper M.J., Design and development of an experimental wrought aluminum alloy for use at elevated temperatures, *Metall. Mater. Trans. A*, 1988, **19** (4): 1027.

[9] Frindlyyander I.N., Translated by Yao Y.Z., *Wrought Structural Aluminum Alloys*, Scientific and Technology Literature Publishing House, Chongqing, 1989: 153.